May 21, 2014

1   Scattering Basics

The incoming and outgoing wavevectors of the x-ray beam in Fig. XXX are given by

$$\mathbf{k}_{\text{in}} = \frac{2\pi}{\lambda}\hat{\mathbf{y}}, \quad \mathbf{k}_{\text{out}} = \frac{2\pi}{\lambda}\left(\sin 2\theta \cos\phi\,\hat{\mathbf{x}} + \cos 2\theta\,\hat{\mathbf{y}} + \sin 2\theta \sin\phi\,\hat{\mathbf{z}}\right), \qquad (1)$$

where λ is the wavelength of x-ray, 2θ is the total scattering angle, and ϕ is the angle measured from the equator on the detector. The scattering vector (also called momentum transfer vector) is the difference between $\mathbf{k}_{\text{in}}$ and $\mathbf{k}_{\text{out}}$,

$$\begin{aligned}\mathbf{q} &= \mathbf{k}_{\text{out}} - \mathbf{k}_{\text{in}} \\ &= q\left(\cos\theta \cos\phi\,\hat{\mathbf{x}} - \sin\theta\,\hat{\mathbf{y}} + \cos\theta \sin\phi\,\hat{\mathbf{z}}\right),\end{aligned} \qquad (2)$$

where $q = 4\pi \sin\theta/\lambda$ is the magnitude of the scattering vector. When the sample is rotated by ω about the lab x-axis in the clockwise direction as shown in Fig. XXX, the sample coordinates differ from the lab coordinates and are given by

$$\hat{\mathbf{e}}_{\mathbf{x}} = \hat{\mathbf{x}}, \quad \hat{\mathbf{e}}_{\mathbf{y}} = \cos\omega\,\hat{\mathbf{y}} + \sin\omega\,\hat{\mathbf{z}}, \quad \hat{\mathbf{e}}_{\mathbf{z}} = -\sin\omega\,\hat{\mathbf{y}} + \cos\omega\,\hat{\mathbf{z}}. \qquad (3)$$

From Eq. (2) and (3), we find the projection of $\mathbf{q}$ on the sample coordinates to be

$$\begin{aligned} q_x &= \mathbf{q}\cdot\hat{\mathbf{e}}_{\mathbf{x}} = q\cos\theta\cos\phi, \\ q_y &= \mathbf{q}\cdot\hat{\mathbf{e}}_{\mathbf{y}} = q\left(-\sin\theta\cos\omega + \cos\theta\sin\phi\sin\omega\right), \\ q_z &= \mathbf{q}\cdot\hat{\mathbf{e}}_{\mathbf{z}} = q\left(\sin\theta\sin\omega + \cos\theta\sin\phi\cos\omega\right). \end{aligned} \qquad (4)$$

The position, (X, Z), of a CCD pixel is measured with respect to the beam and given by

$$X = S\tan 2\theta \cos\phi, \quad Z = S\tan 2\theta \sin\phi, \qquad (5)$$

where S is the distance between the sample and detector. From a model for the electron density of a lipid bilayer, one calculates a X-ray scattering intensity pattern, $I(\mathbf{q})$. Then, Eq. (4) and (5) relate $I(\mathbf{q})$ to the experimentally measured intensity pattern, $I(X, Z)$. It is important to remember that

1

a given pixel position, (X, Z), corresponds to a triplet (q_x, q_y, q_z). Fully exploring the sample q-space requires changing ω for a fixed wavelength, which was achieved by continuously rotating the sample with a motor. In the ripple phase, because our sample has in-plane rotational symmetry, the ripple side peaks make up Bragg rings while the main peaks are still delta function like (see Fig. X) in q-space. In order for the main peak to be observed, ω must be equal to θ_{B}, but the side peaks are observed at any ω. Those side peaks get slightly smeared due to integration over q_y.

For low angle x-ray scattering (LAXS), it is convenient to linearize the above equations in terms of θ and ω. In the small angle approximation, $\sin \phi \approx Z/(2S\theta)$ and $\cos \phi \approx X/(2S\theta)$, and

$$
\begin{aligned}
q_x &\approx \frac{4\pi\theta \cos \phi}{\lambda} \approx kX/S \\
q_y &\approx q_z\omega - \frac{4\pi\theta^2}{\lambda} \approx q_z\omega - \frac{\lambda q_z^2}{4\pi} \\
q_z &\approx \frac{4\pi\theta \sin \phi}{\lambda} \approx kZ/S,
\end{aligned}
\tag{6}
$$

with $k = 2\pi/\lambda$. For wide angle X-ray scattering, the exact relations given by Eq. (4) are necessary. Especially in the transmission experiment, where ω is large, an observed X-ray pattern appears nontrivial and becomes almost impossible to analyze without the use of Eq. (4).

2 Geometric Correction for the Ripple Phase Scattering

In order to capture both main and side peaks in one x-ray exposure, the sample was continuously rotated. As a result of the rotation, the main peaks become arcs that subtend an angle $2\theta_h$, as shown in Fig. 1, with its length equal to $2\theta_h q_{z,h}$. What is recorded on the detector is the cross section of this arc with the Ewald sphere, so the total intensity is the product of the observed intensity with the arc length, that is,

$$
I = 2\theta_h q_{z,h} I_{\mathrm{o},h}.
\tag{7}
$$

Because the sample has in-plane rotational symmetry, the side peaks turn into Bragg rings whose radius is $q_{r,k}$, as shown in Figure X. These rings cross
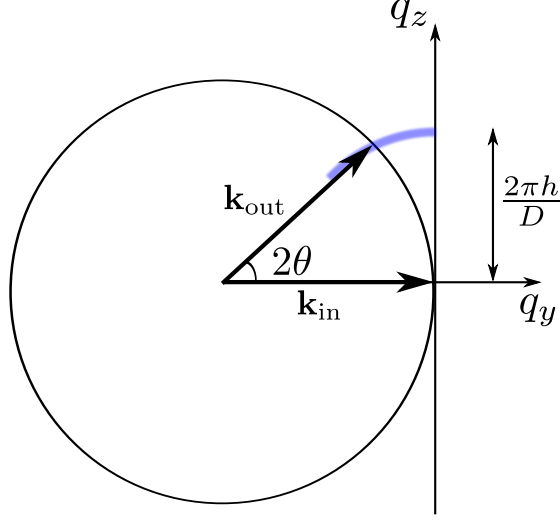
Figure 1: caption goes here

the Ewald sphere at all angles of ω. Then, the total intensity is given by

$$I = 2\pi q_{r,k} I_{\text{o},k}. \tag{8}$$

Inverting Eq. (7) and (8) and realizing that the intensity is the form factor squared, we can calculate the observed intensity, I_o, from a model for electron density in the ripple phase.

Mathematically, the rotation is equivalent to an integration over ω. In low angle X-ray scattering, q_z is constant at a given pixel as ω is changed, which can be seen from Eq. (6). ω dependence appears only through q_y, so rotating the sample is realized by integrating over q_y. To derive the integration limits, let us consider two cases: (a) When $\omega \leq 0$, the incoming X-ray beam is blocked by the back of the substrate. This sets the lower limit to 0. (b) When $\omega \geq 2\theta$, the substrate blocks the outgoing X-ray. Within the small angle approximation, then, ω_{max} is $2 \times \lambda q_z/(4\pi)$. Thus, the integration limits for q_y integration are $[-\lambda q_z^2/(4\pi), \lambda q_z^2/(4\pi)]$. We also need to integrate over X and Z to obtain integrated intensity. These lead to the observed intensity

3

written as,

$$I_{\mathrm{o},hk} \propto \int dX \int dZ \int d\omega |F_{hk}|^2 S_{hk}(\mathbf{q})$$

$$\propto |F_{hk}|^2 \int dq_x \int dq_z \int_{-\frac{\lambda q_z^2}{4\pi}}^{\frac{\lambda q_z^2}{4\pi}} \frac{dq_y}{q_z} S_{hk}(\mathbf{q}), \tag{9}$$

where $1/q_z$ factor in q_y integration is the Lorentz polarization factor in the small angle approximation.

For a crystalline sample with the in-plane rotational symmetry, the structure factor is

$$S_{hk}(\mathbf{q}) = S_{hk}(q_r, q_z) = \frac{1}{2\pi q_r} \delta(q_r - q_{r,k}) \delta(q_z - q_{z,hk}), \tag{10}$$

where $q_{r,k} = 2\pi |k|/\lambda_r$. Thus, the scattering pattern in the ripple phase is a collection of Bragg "rings" centered at the meridian and the Bragg peaks that are called the main peaks.

The observed, integrated intensity of hk peak is proportional to

$$I_{\mathrm{o},hk} \propto \frac{|F_{hk}|^2}{q_{z,hk}} \int dq_x \int_{-q_{y0}}^{q_{y0}} dq_y \frac{\delta(q_r - q_{r,k})}{2\pi q_r}, \tag{11}$$

where $q_{y0} = \lambda q_{z,hk}^2/(4\pi)$. For side peaks $(k \neq 0)$, we have

$$\int dq_x \int_{-q_{y0}}^{q_{y0}} dq_y \frac{\delta(q_r - q_{r,k})}{2\pi q_r} \approx \int_{-\frac{q_{y0}}{q_{r,k}}}^{\frac{q_{y0}}{q_{r,k}}} d\phi \int dq_r \, q_r \frac{\delta(q_r - q_{r,k})}{2\pi q_r}$$

$$= \frac{q_{y0}}{\pi q_{r,k}}. \tag{12}$$

For the main peaks $(k = 0)$, we have

$$\int dq_x \int_{-q_{y0}}^{q_{y0}} dq_y \frac{\delta(q_r - q_{r,k})}{2\pi q_r} = \int_0^{2\pi} d\phi \int dq_r \, q_r \frac{\delta(q_r - q_{r,k})}{2\pi q_r}$$

$$= 1 \tag{13}$$

Using Eq. () and (), we write the observed integrated intensity as

$$I_{\mathrm{o},h0} \propto \frac{|F_{h0}|^2}{q_{z,h0}} \tag{14}$$

$$I_{\mathrm{o},hk} \propto \frac{|F_{hk}|^2}{q_{z,hk}} \frac{q_{y0}}{\pi q_{r,k}} = |F_{hk}|^2 \frac{\lambda q_{z,hk}}{2\pi} \frac{1}{2\pi q_{r,k}} = |F_{hk}|^2 \frac{2\theta_{hk}}{2\pi q_{r,k}}, \tag{15}$$

4

where $2\theta_{hk} = \lambda q_{z,hk}/(2\pi)$ is the incident angle at which the outgoing x-ray with its scattering angle equal to θ_{hk} gets blocked by the substrate. Eq. (14) and (15) relate the form factor calculated from a model to the experimentally observed intensity, and are equivalent to Eq. (7) and (8), which were derived by using the Ewald sphere.

In non linear least square fitting procedure, we fitted the observed integrated intensity to the calculated intensity from a bilayer model using these geometrical corrections. This is mainly due to our ability to determine the experimental uncertainties on observed intensity rather than the geometrically corrected form factor. Fitting observed intensity is simpler because it allows us to avoid propagating the uncertainties.

3   Sawtooth model

The unit cell vectors in the ripple phase can be expressed as

$$\mathbf{a} = \frac{D}{\tan\gamma}\hat{\mathbf{x}} + D\hat{\mathbf{z}} \tag{16}$$

and

$$\mathbf{b} = \lambda_r\hat{\mathbf{x}}. \tag{17}$$

The corresponding reciprocal lattice unit cell vectors are given by

$$\mathbf{A} = \frac{2\pi}{D}\hat{\mathbf{z}} \tag{18}$$

and

$$\mathbf{B} = \frac{2\pi}{\lambda_r}\hat{\mathbf{x}} - \frac{2\pi}{\lambda_r\tan\gamma}\hat{\mathbf{z}}. \tag{19}$$

The reciprocal lattice vector, $\mathbf{q}_{hk}$ for the Bragg peak with Miller indices (h,k) is

$$\mathbf{q}_{hk} = h\mathbf{A} + k\mathbf{B}, \tag{20}$$

so its components can be written as

$$q_{x,k} = \frac{2\pi k}{\lambda_r} \tag{21}$$

$$q_y = 0 \tag{22}$$

$$q_{z,hk} = \frac{2\pi h}{D} - \frac{2\pi k}{\lambda_r\tan\gamma} \tag{23}$$

4   Data

Figure shows a LAXS pattern from DMPC at 18 °C. $D = 57.9$ Å. Low resolution experiment. Up to $h = 9$ orders were observed in this data set. Because of a non-negligible degree of mosaicity in the sample, strong orders cast their arcs over weaker orders. A care must be taken to decompose the intensity at a given pixel to intensity due to a strong order's arc and to that due to a weak peak. This was achieved by taking a q_z swath and fitting the intensity to two Gaussian functions whose widths were determined from the known instrumental resolution. Figure shows an example of this operation. Table and Table show with and without the decomposition operation, respectively. For many of the orders observed, errors one would expect from neglecting the mosaicity effect were small. For higher orders, however, this was crucial to obtain the correct integrated intensity.

In order to test the decomposition effect, fits were also performed for the sum of intensity for orders that overlap.

First, we fitted the data using only up to $h = 3$ orders. What did we get? How did each model do? Any inconsistency with Sun PNAS?

Next, we fitted every peak we observed. Which model failed?

5   Contour Part of the Form Factor

As in ref, we take the ripple profile to have a sawtooth-like profile. Its amplitude is $A/2$ and the projection of the major arm on the ripple direction is x_0 as shown in Fig. X. Then, we write the ripple profile as

$$u(x) = \begin{cases} -\frac{A}{\lambda_r - x_0}\left(x + \frac{\lambda_r}{2}\right) & \text{for} \quad -\frac{\lambda_r}{2} \le x < -\frac{x_0}{2}, \\ \frac{A}{x_0}x & \text{for} \quad -\frac{x_0}{2} \le x \le \frac{x_0}{2}, \\ -\frac{A}{\lambda_r - x_0}\left(x - \frac{\lambda_r}{2}\right) & \text{for} \quad \frac{x_0}{2} < x \le \frac{\lambda_r}{2}. \end{cases} \tag{24}$$

The ripple profile has the inversion symmetry, so that the resulting form factor is real. A and x_0 are fitting parameters that depend on the integrated intensity of each peak while D and λ_r are determined from measuring the positions of the Bragg peaks.

In order to allow the electron density along the ripple direction to modulate, we include two additional parameters, one to allow for the electron density across the minor side to be different by a ratio f_1 from the electron density across the major side and a second parameter f_2, which is multiplied

by δ functions $\delta(x \pm x_0/2)$ to allow for a different electron density near the kink between the major and the minor sides.

6 Delta Function Model

7 2G Hybrid Model

In the hybrid model, the terminal methyl region of the bilayer is represented as a Gaussian function [1]. The headgroups are represented by one and two Gaussian functions in 1G and 2G hybrid model, respectively. The methylene and water regions are each treated as a constant. The gap between the two constants is represented by a sine function. Then, for half of the bilayer, $0 \le z \le D/2$, the electron density has the form,

$$\rho(z) = \rho_G(z) + \rho_S(z) + \rho_B(z), \tag{25}$$

where the Gaussian part is given by

$$\rho_G(z) = \sum_{i=1}^{1 \text{ or } 2} \rho_{Hi} e^{-(z-Z_{Hi})^2/(2\sigma_{Hi}^2)} + \rho_M e^{-z^2/(2\sigma_M^2)}, \tag{26}$$

the strip part is given by

$$\rho_S(z) = \begin{cases} \rho_{CH_2} & \text{for} \quad 0 \le z < Z_{CH_2}, \\ \rho_W & \text{for} \quad Z_W \le z \le D/2, \end{cases} \tag{27}$$

and the bridging part is given by

$$\rho_B(z) = \frac{\rho_W - \rho_{CH_2}}{2} \cos\left[\frac{-\pi}{\Delta Z_H}(z - Z_W)\right] + \frac{\rho_W + \rho_{CH_2}}{2} \quad \text{for} \quad Z_{CH_2} < z < Z_W. \tag{28}$$

with $\Delta Z_H = Z_W - Z_{CH_2}$. Here, we assume $Z_{H2} > Z_{H1}$. Table 1 shows some of the definitions. The transbilayer profile along $x = -z \tan \psi$ can be obtained by rotating the coordinates x and z by ψ in the clockwise direction and reexpressing $\rho(z)$ in terms of the rotated coordinates. This leads to replaincg x with $x' = x \cos \psi + z \sin \psi$ and z with $z' = -x \sin \psi + z \cos \psi$. Then, the rotated transbilayer profile is

$$\rho(x, z) = \delta(x + z \tan \psi)[\rho_G(z') + \rho_S(z') + \rho_B(z')]. \tag{29}$$

	1G	2G
$Z_{\mathrm{CH_2}}$	$Z_{\mathrm{H1}} - \sigma_{\mathrm{H1}}$	$Z_{\mathrm{H1}} - \sigma_{\mathrm{H1}}$
Z_{W}	$Z_{\mathrm{H1}} + \sigma_{\mathrm{H1}}$	$Z_{\mathrm{H2}} + \sigma_{\mathrm{H2}}$

Table 1: Definitions of $Z_{\mathrm{CH_2}}$ and Z_{W}

Taking the two dimensional Fourier transform of Eq. (29) leads to the transbilayer part of the form factor,

$$F_{\mathrm{T}} = \int_{-\frac{D}{2}}^{\frac{D}{2}} \int_{-\frac{\lambda_r}{2}}^{\frac{\lambda_r}{2}} [\rho(x,z) - \rho_{\mathrm{W}}] e^{i(q_x x + q_z z)} dx\,dz \qquad (30)$$

$$= F_{\mathrm{G}} + F_{\mathrm{S}} + F_{\mathrm{B}}. \qquad (31)$$

The form factor is calculated in the minus fluid convention, where the bilayer electron density is measured with respect to the electron density of the surrounding solvent. The expression for F_{T} is rather messy and not shown. The derivation and full expression can be found in the appendix. Here, we note that the fitting parameters in this model are $Z_{\mathrm{H}i}$, $\sigma_{\mathrm{H}i}$, and $R_{\mathrm{H}i\mathrm{M}}$ for each of the two headgroup Gaussian functions, σ_{M} for the terminal methyl Gaussian, ΔR for the methylene region, ψ for the lipid tilt, and an overall scaling factor. The contour part of the form factor has four more parameters (A, x_0, f_1, and f_2). In total, the modified 2G hybrid model implements 14 structural parameters.

8 Electron Density Profile

Table X shows the best fit for each model. It shows that the delta function model fails. Its failure is obviously due to its lack of fine structural details. In ref. (SUN), the model marginally worked because only up to the third orders were available. With the high flux synchrotron X-ray beam, many more higher orders were observed, whose intensity is dominated by finer details in the bilayer electron density. The table shows that 1G model also fails. 2G model works, but simple 2G model failed. $k = 6$ orders clearly require the modulation in the electron density along the ripple direction. The phase of lower orders tends to be the same throughout the different models while higher orders vary widely. These are just ideas. I need to do actual fitting.

A   Rotation of a Two-Dimensional Function

Let us consider rotating a function, $f(x, z)$ in two dimensions by an angle, ψ, in the counterclockwise direction (see Fig. X). This is easily achieved by rotating the coordinate system by ψ in the clockwise direction. Let rotated coordinates be x' and z'. A point in the original coodinates, (x, z), is written as (x', z') in the new coordinates. More specifically, the point P is written as $\mathbf{P} = x\hat{\mathbf{x}} + z\hat{\mathbf{z}} = x'\hat{\mathbf{x}}' + z'\hat{\mathbf{z}}'$. $\hat{\mathbf{x}}$ and $\hat{\mathbf{z}}$ in the $x'z'$ coordinate system are written as

$$\hat{\mathbf{x}} = \cos\psi\hat{\mathbf{x}}' + \sin\psi\hat{\mathbf{z}}' \tag{32}$$
$$\hat{\mathbf{z}} = -\sin\psi\hat{\mathbf{x}}' + \cos\psi\hat{\mathbf{z}}'. \tag{33}$$

Pluggin these in $\mathbf{P} = x\hat{\mathbf{x}} + z\hat{\mathbf{z}}$ leads to

$$x' = x\cos\psi - z\sin\psi \tag{34}$$
$$z' = z\cos\psi + x\sin\psi, \tag{35}$$

the inverse of which is

$$x = x'\cos\psi + z'\sin\psi \tag{36}$$
$$z = -x'\sin\psi + z'\cos\psi. \tag{37}$$

Using the latter equations, $f(x, z)$ can be expressed in terms of x' and z'. The resulting function $f(x', z')$ is the rotated version of $f(x, z)$.

As an example, let us consider a Dirac delta function located at $(x, z) = (0, Z_{\mathrm{H}})$, that is, $f(x, z) = \delta(x)\delta(z - Z_{\mathrm{H}})$. After the rotation by ψ, it becomes

$$
\begin{aligned}
f(x, z) &\to \delta(x\cos\psi + z\sin\psi)\delta(-x\sin\psi + z\cos\psi - Z_{\mathrm{H}}) \\
&= \frac{\delta(x + z\tan\psi)}{|\cos\psi|}\frac{\delta(-x\sin\psi\cos\psi + z\cos^2\psi - Z_{\mathrm{H}\cos}\psi)}{1/|\cos\psi|} \\
&= \delta(x + z\tan\psi)\delta(z\tan\psi\sin\psi\cos\psi + z\cos^2\psi - Z_{\mathrm{H}\cos}\psi) \\
&= \delta(x + z\tan\psi)\delta(z - Z_{\mathrm{H}\cos}\psi),
\end{aligned}
$$

which is a part of the expression for $T_\psi(x, z)$ in the simple delta function model.

B Derivation of the transbilayer part of the form factor in the 2G hybrid model

In this section, we derive the trasbilayer part of the form factor calculated from the 2G hybrid model discussed in section X. Defining $z' = -x \sin \psi + z \cos \psi$, the Fourier transform of a Gaussian function along the line tilted from z-axis by ψ is

$$
\iint dz\, dx\, \rho_{\mathrm{H}i} \exp\left\{-\frac{(z' - Z_{\mathrm{H}i})^2}{2\sigma_{\mathrm{H}i}^2}\right\} \delta(x \cos \psi + z \sin \psi) e^{iq_x x} e^{iq_z z}
$$

$$
= \frac{1}{\cos \psi} \int_{-\frac{D}{2}}^{\frac{D}{2}} dz\, \rho_{\mathrm{H}i} \exp\left\{-\frac{(z - Z_{\mathrm{H}i} \cos \psi)^2}{2\sigma_{\mathrm{H}i}^2 \cos^2 \psi} + i(q_z - q_x \tan \psi)z\right\}
$$

$$
\approx \rho_{\mathrm{H}i} \sqrt{2\pi} \sigma_{\mathrm{H}i} \exp\left\{i\alpha Z_{\mathrm{H}i} - \frac{1}{2}\alpha^2 \sigma_{\mathrm{H}i}^2\right\} \tag{38}
$$

with $\alpha = q_z \cos \psi - q_x \sin \psi$. Using Eq. (38) and adding the other side of the bilayer and the terminal methyl term, we get

$$
F_{\mathrm{G}} = \sqrt{2\pi}\left[-\rho_{\mathrm{M}}\sigma_{\mathrm{M}} \exp\left\{-\frac{1}{2}\alpha^2 \sigma_{\mathrm{M}}^2\right\}\right.
$$

$$
\left. + \sum_{i=1}^{1 \text{ or } 2} 2\rho_{\mathrm{H}i}\sigma_{\mathrm{H}i} \cos(\alpha Z_{\mathrm{H}i}) \exp\left\{-\frac{1}{2}\alpha^2 \sigma_{\mathrm{H}i}^2\right\}\right]. \tag{39}
$$

The strip part of the model in the minus fluid convention is

$$
\rho_{\mathrm{S}}(z) = \begin{cases} -\Delta\rho & \text{for} \quad 0 \leq z < Z_{\mathrm{CH}_2} \cos \psi, \\ 0 & \text{for} \quad Z_{\mathrm{W}} \cos \psi \leq z \leq D/2, \end{cases} \tag{40}
$$

where $\Delta\rho = \rho_{\mathrm{W}} - \rho_{\mathrm{CH}_2}$. Then, the corresponding Fourier transform is

$$
F_{\mathrm{S}} = \iint dz\, dx\, e^{iq_x x} e^{iq_z z} \rho_{\mathrm{S}}(z)\delta(x \cos \psi + z \sin \psi)
$$

$$
= \frac{2}{\cos \psi} \int_0^{Z_{\mathrm{CH}_2} \cos \psi} dz \cos\left(\frac{\alpha}{\cos \psi}z\right)(-\Delta\rho)
$$

$$
= -2\Delta\rho\frac{\sin(\alpha Z_{\mathrm{CH}_2})}{\alpha}. \tag{41}
$$

10

The bridging part of the model in the minus fluid convention is

$$\rho_B(x, z) = \frac{\Delta\rho}{2} \cos\left[\frac{-\pi}{\Delta Z_H}(z' - Z_W)\right] - \frac{\Delta\rho}{2} \tag{42}$$

for $Z_{CH_2} \cos\psi < z < Z_W \cos\psi$, and 0 otherwise. Here, $\Delta Z_H = Z_W - Z_{CH_2}$. Then, for the strip part of the form factor, we have

$$
\begin{aligned}
F_B &= \iint dz\, dx\, e^{iq_x x} e^{iq_z z} \delta(x \cos\psi + z \sin\psi)\rho_B(x, z) \\
&= \frac{\Delta\rho}{\cos\psi} \int_{Z_{CH_2}\cos\psi}^{Z_W\cos\psi} dz \cos\left(\alpha \frac{z}{\cos\psi}\right)\left\{\cos\left[-\frac{\pi}{\Delta Z_H}\left(\frac{z}{\cos\psi} - Z_W\right)\right] - 1\right\} \\
&= \Delta\rho \left\{\frac{\Delta Z_H \sin\left[\frac{\pi(-u + Z_W)}{\Delta Z_H} + \alpha u\right]}{-2\pi + 2\alpha\Delta Z_H} + \frac{\Delta Z_H \sin\left[\frac{\pi(u - Z_W)}{\Delta Z_H} + \alpha u\right]}{2\pi + 2\alpha\Delta Z_H} - \frac{\sin(\alpha u)}{\alpha}\right\}\Bigg|_{Z_{CH_2}}^{Z_W} \\
&= -\frac{\Delta\rho}{\alpha}[\sin(\alpha Z_W) - \sin(\alpha Z_{CH_2})] \\
&\quad + \frac{\Delta\rho}{2}\left(\frac{1}{\alpha + \frac{\pi}{\Delta Z_H}} + \frac{1}{\alpha - \frac{\pi}{\Delta Z_H}}\right)[\sin(\alpha Z_W) + \sin(\alpha Z_{CH_2})]. \tag{43}
\end{aligned}
$$

Because our X-ray scattering intensity was measured in a relative scale, an overall scaling factor was necessary for a non linear least square fitting procedure. This means that $\Delta\rho$ can be absorbed in the scaling factor. Doing so means that the values of ρ_{Hi} and ρ_M resulting from a fitting procedure are relative to $\Delta\rho$. One way to have these parameters in the absolute scale is to integrate the bilayer electron density over the lipid volume and equate the result to the total number of electrons in the lipid, which can easily be calculated from the chemical formula. For the ripple phase study in this thesis, the absolute values of the electron density were not of importance, so the discussion was omitted in the main text.

C Derivation of the contour part of the form factor

In this section, we derive F_{C}. The ripple profile, $u(x)$ is given by

$$u(x) = \begin{cases} -\frac{A}{\lambda_r - x_0}\left(x + \frac{\lambda_r}{2}\right) & \text{for} & -\frac{\lambda_r}{2} \le x < -\frac{x_0}{2} \\ \frac{A}{x_0}x & \text{for} & -\frac{x_0}{2} \le x \le \frac{x_0}{2} \\ -\frac{A}{\lambda_r - x_0}\left(x - \frac{\lambda_r}{2}\right) & \text{for} & \frac{x_0}{2} < x \le \frac{\lambda_r}{2} \end{cases} \tag{44}$$

The contour part of the form factor is the Fourier transform of the contour function, $C(x, z)$,

$$F_{\mathrm{C}}(\mathbf{q}) = \frac{1}{\lambda_r} \int_{-\frac{\lambda_r}{2}}^{\frac{\lambda_r}{2}} dx \int_{-\frac{D}{2}}^{\frac{D}{2}} dz\, C(x, z) e^{iq_z z} e^{iq_x x}$$

As discussed in section X, the modulated models allow the electron density to modulate along the ripple direction, x. This means

$$C(x, z) = \begin{cases} f_1 \delta[z - u(x)] & \text{for} & -\frac{\lambda_r}{2} \le x < -\frac{x_0}{2} \\ \delta[z - u(x)] & \text{for} & -\frac{x_0}{2} < x < \frac{x_0}{2} \\ f_1 \delta[z - u(x)] & \text{for} & \frac{x_0}{2} \le x < \frac{\lambda_r}{2} \end{cases}$$
$$+ f_2\, \delta\left(x + \frac{x_0}{2}\right)\delta\left(z + \frac{A}{2}\right) + f_2\, \delta\left(x - \frac{x_0}{2}\right)\delta\left(z - \frac{A}{2}\right). \tag{45}$$

The contribution from the minor arm is

$$\frac{1}{\lambda_r}\int_{-\frac{\lambda_r}{2}}^{-\frac{x_0}{2}} dx\, e^{iq_x x} e^{iq_z u(x)} + \int_{\frac{x_0}{2}}^{\frac{\lambda_r}{2}} dx\, e^{iq_x x} e^{iq_z u(x)}$$

$$= \frac{1}{\lambda_r}\int_{\frac{x_0}{2}}^{\frac{\lambda_r}{2}} dx\, e^{-i\left[q_x x - q_z \frac{A}{\lambda_r - x_0}\left(x - \frac{\lambda_r}{2}\right)\right]} + \int_{\frac{x_0}{2}}^{\frac{\lambda_r}{2}} dx\, e^{i\left[q_x x - q_z \frac{A}{\lambda_r - x_0}\left(x - \frac{\lambda_r}{2}\right)\right]}$$

$$= \frac{2}{\lambda_r}\int_{\frac{x_0}{2}}^{\frac{\lambda_r}{2}} \cos\left[\left(q_x - q_z \frac{A}{\lambda_r - x_0}\right)x + q_z \frac{A}{\lambda_r - x_0}\frac{\lambda_r}{2}\right] \tag{46}$$

Using a trigonometric identity,

$$\sin u - \sin v = 2\cos[(u + v)/2]\sin[(u - v)/2],$$

and defining

$$\omega(\mathbf{q}) = \frac{1}{2}\left(q_x x_0 + q_z A\right), \tag{47}$$

we further simplify Eq. (46),

$$
\begin{aligned}
&= \frac{2}{\lambda_r} \frac{\lambda_r - x_0}{\frac{1}{2}q_x\lambda_r - \omega} \cos\left[\frac{1}{2}\left(\frac{1}{2}q_x\lambda_r + \omega\right)\right] \sin\left[\frac{1}{2}\left(\frac{1}{2}q_x\lambda_r - \omega\right)\right] \\
&= \frac{1}{\lambda_r} \frac{\lambda_r - x_0}{\frac{1}{2}q_x\lambda_r - \omega} \cos\left[\frac{1}{2}\left(\frac{1}{2}q_x\lambda_r + \omega\right)\right] \frac{\sin\left(\frac{1}{2}q_x\lambda_r - \omega\right)}{\cos\left[\frac{1}{2}\left(\frac{1}{2}q_x\lambda_r - \omega\right)\right]} \\
&= \frac{\lambda_r - x_0}{\lambda_r} \frac{\cos\left[\frac{1}{2}\left(\frac{1}{2}q_x\lambda_r + \omega\right)\right]}{\cos\left[\frac{1}{2}\left(\frac{1}{2}q_x\lambda_r - \omega\right)\right]} \frac{\sin\left(\frac{1}{2}q_x\lambda_r - \omega\right)}{\frac{1}{2}q_x\lambda_r - \omega}.
\end{aligned}
\tag{48}
$$

Similarly, we calculate the contribution from the major arm,

$$
\begin{aligned}
\frac{1}{\lambda_r} \int_{-\frac{x_0}{2}}^{\frac{x_0}{2}} dx\, e^{i\left(\frac{q_z A}{x_0} + q_x\right)x} &= \frac{2}{\lambda_r} \int_0^{\frac{x_0}{2}} dx \cos\left(\frac{q_z A}{x_0} + q_x\right)x \\
&= \frac{x_0}{\lambda_r} \frac{\sin\omega}{\omega}
\end{aligned}
\tag{49}
$$

The contribution from the kink region is

$$
\begin{aligned}
&\frac{1}{\lambda_r} \iint dx\, dz \left[\delta\left(x + \frac{x_0}{2}\right)\delta\left(z + \frac{A}{2}\right) + \delta\left(x - \frac{x_0}{2}\right)\delta\left(z - \frac{A}{2}\right)\right] e^{iq_x x} e^{iq_z z} \\
&= \frac{2}{\lambda_r} \cos\omega.
\end{aligned}
\tag{50}
$$

Therefore,

$$
\begin{aligned}
F_{\mathrm{C}}(\mathbf{q}) &= \frac{x_0}{\lambda_r}\frac{\sin\omega}{\omega} + f_1 \frac{\lambda_r - x_0}{\lambda_r} \frac{\cos\left[\frac{1}{2}\left(\frac{1}{2}q_x\lambda_r + \omega\right)\right]}{\cos\left[\frac{1}{2}\left(\frac{1}{2}q_x\lambda_r - \omega\right)\right]} \frac{\sin\left(\frac{1}{2}q_x\lambda_r - \omega\right)}{\frac{1}{2}q_x\lambda_r - \omega} \\
&\quad + \frac{2f_2}{\lambda_r}\cos\omega
\end{aligned}
\tag{51}
$$

D Correction due to refractive index

q_z needs be corrected for index of refraction. Let θ' and λ' be the true scattering angle and wavelength within the sample. The wavelength by an energy analyzer, λ, and the scattering angle calculated from a position on a CCD detector, θ are apparent. The correction is not necessary in the horizontal direction. The Snell's law in Fig. X gives

$$
n\cos\theta = n'\cos\theta'
\tag{52}
$$

$$
n\lambda = n'\lambda'.
\tag{53}
$$

13

For low angle X-ray scattering, the momentum transfer along z direction is

$$q_z = \frac{4\pi \sin \theta'}{\lambda'} \tag{54}$$

$$= \frac{4\pi n'}{n\lambda} \sin \theta' \tag{55}$$

$$= \frac{4\pi n'}{n\lambda} \sqrt{1 - \cos^2 \theta'} \tag{56}$$

$$= \frac{4\pi n'}{n\lambda} \sqrt{1 - \left(\frac{n}{n'} \cos \theta\right)^2}. \tag{57}$$

The apparent scattering angle, θ, is directly related to the vertical pixel position, p_z, by

$$\theta = \frac{1}{2} \tan^{-1} \left(\frac{p_z}{S}\right), \tag{58}$$

where S is the sample-to-detector distance. The typical units of S and p_z are in mm. In our experimental setup, $n = 1$ and $n' = 0.9999978$ for lipids at $\lambda = 1.18$ Å.

References

[1] M.C. Wiener, R.M. Suter, and J.F. Nagle. Structure of the fully hydrated gel phase of dipalmitoylphosphatidylcholine. *Biophysical Journal*, 55(2):315 – 325, 1989.